Biomedical Signal Processing and Control 8 (2013) 901–908

Contents lists available at ScienceDirect

Biomedical Signal Processing and Control

journal homepage: www.elsevier.com/locate/bspc

Short communication

Analysis and classification of speech imagery EEG for BCI

Li Wang*, Xiong Zhang, Xuefei Zhong, Yu Zhang

School of Electronic Science and Engineering, Southeast University, Nanjing 210096, China

ARTICLE INFO

Article history:
Received 10 December 2012
Received in revised form 22 July 2013
Accepted 31 July 2013
Available online 21 September 2013

Keywords:
Brain–computer interface (BCI)
Common spatial patterns (CSP)
Electroencephalogram (EEG)
Speech imagery
Support vector machine (SVM)

ABSTRACT

Electroencephalogram (EEG) is generally used in brain–computer interface (BCI), including motor imagery, mental task, steady-state evoked potentials (SSEPs) and P300. In order to complement existing motor-based control paradigms, this paper proposed a novel imagery mode: speech imagery. Chinese characters are monosyllabic and one Chinese character can express one meaning. Thus, eight Chinese subjects were required to read two Chinese characters in mind in this experiment. There were different shapes, pronunciations and meanings between two Chinese characters. Feature vectors of EEG signals were extracted by common spatial patterns (CSP), and then these vectors were classified by support vector machine (SVM). The accuracy between two characters was not superior. However, it was still effective to distinguish whether subjects were reading one character in mind, and the accuracies were between 73.65% and 95.76%. The results were better than vowel speech imagery, and they were suitable for asynchronous BCI. BCI systems will be also extended from motor imagery to combine motor imagery and speech imagery in the future.

© 2013 Elsevier Ltd. All rights reserved.

1. Introduction

Brain–computer interface (BCI) research is advancing very rapidly. It provides a new non-muscular channel for patients with motor dysfunction [1], such as amyotrophic lateral sclerosis (ALS), stroke, spinal cord injury, and traumatic brain injury, to exchange information with the external world. As it directly provides a new information exchange and control path for the users, which bypasses the peripheral nerve and muscle tissue, the quality of users' life can be improved greatly. BCI research has been arisen around the world over the past 25 years with decreasing the cost of electronic equipment, especially that the technology based on classifying single trial electroencephalography (EEG) has been attracted enough attention by researchers. There are some potential applications of BCI, for example, movement within virtual reality environments, computer cursors and virtual keyboards operation for disabled person.

Several BCI methods have been developed, such as EEG [2], magnetoencephalography (MEG) [3], electrocorticography (ECoG) [4], functional magnetic resonance imaging (fMRI) [5], and near-infrared spectroscopy (NIRS) [6]. As EEG is a non-invasive technology and it is much cheaper than others, the BCI systems based on EEG have been studied widely. EEG signals can be varied by several brain activities, e.g. event-related (de)synchronization (ERD/ERS) [7], mental task [8], steady-state evoked potentials (SSEPs) [9], and P300 evoked potentials [10]. ERD/ERS of sensory-motor rhythms are found during overt motor execution and motor imagery. To the best of our knowledge, the motor imagery-based BCI provides high classification accuracy, but its maximum number of categories is only four [11]. It is not very convenient to use SSEPs and P300 BCIs, as they depend on additional equipment to produce stimuli. Furthermore, users may feel fatigue after using long time.

For the above reasons, a novel speech imagery BCI system is proposed. Eric C Leuthardt had used ECoG speech network to control a BCI [12], and DaSalla proposed /a/ and /u/ as vowel speech imageries for EEG-based BCI [13]. In this paper, it is the first time to analyze and classify EEG signals from characters speech imagery. These characters had specific meaning. Chinese characters are monosyllabic, and one Chinese character can express one meaning. For example, "左" is pronounced as "zuo" in third tone, and it means left in English; "壹" is pronounced as "yi" in first tone, and it means one in English. As "左(left)" and "壹(one)" have different pronunciations, shapes and meanings and they are very commonly used in daily life, they are selected as the characters of speech imagery. We tried to use common spatial patterns (CSP) and support vector machine (SVM) to separate EEG signals when subjects were reading Chinese characters in mind.

2. Methods

2.1. Subjects and experimental paradigm

The datasets were recorded from eight healthy, right-handed Chinese subjects (two females and six males) in the no feedback

* Corresponding author. Tel.: +86 13813363667; fax: +86 25 84536903.
E-mail address: 230119219@seu.edu.cn (L. Wang).

1746-8094/$ – see front matter © 2013 Elsevier Ltd. All rights reserved.
http://dx.doi.org/10.1016/j.bspc.2013.07.011

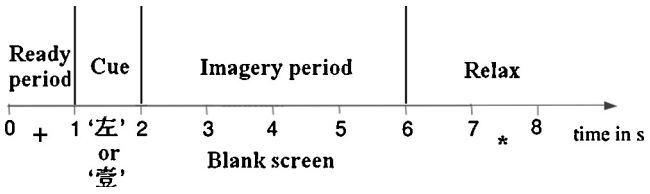

Fig. 1. Timing of a trial of the training paradigm. 3–5 s of every trial, and 2 s of relax period after imagery period of each Chinese character is regarded as Rest. These two fragments of EEG data are separated by CSP spatial filters and SVM classifier.

experiment. Their ages were from 22 to 27 with the average of 23.14 years, and the standard deviation of 1.46 years. All of the subjects did not attend similar experiment before, except that two of them had even been trained in motor imagery experiment. They were seated on a comfortable chair in front of a LCD monitor with 1 m distance, and their arms were relaxed rested on the arm of the chair. Purpose and instructions of the experiment were explained to subjects, and then they signed Informed Consent. The experiment was under the guidance of the Academic Ethics Committee of Southeast University.

The training paradigm includes a repetition of cue-based trials of two different Chinese characters. Timing is shown in Fig. 1. At the beginning of each trial, a fixation cross is displayed with black background, which suggests ready period of 1 s. After the ready period, a Chinese character ("左" or "壹") appears for 1 s on the screen. Each Chinese character will be read in mind by the subjects in the next period. Between 2 and 6 s, Chinese character disappears and the screen displays black background. As it is very fast to read a Chinese character in mind one time, subjects are asked to keep up reading it in mind over and over within the 4 s. In this period, subjects should not move lips or make a sound. After 6 s (at $t = 6$ s), in order to prevent the subjects to adapt the experiment, a fixation asterisk is displayed for 2–3 s with black background, which suggests that they can have a rest after the imagery period. Each of two Chinese characters is randomly displayed 15 times in each run, and the subsequent analysis of EEG data includes a total of five runs in this paper for each subject. Between each run, subjects have a break of 5 min. Overall, there are 150 trials for each subject, so each Chinese character has 75 trials.

2.2. Data acquisition

As speech is the brain's higher cognitive behavior, it involves wide range of distributed network of cortical areas [14]. One general point of view is that speech is mainly processed by the left hemispheric, which includes two regions. One region is located in the posterior-superior temporal lobe, called Wernicke's area, and another one is located in the posterior-inferior frontal gyrus, called Broca's area [15]. In this paper, EEG signals are recorded by a SynAmps 2 system (Neuroscan Co., Ltd.) from two different electrode distributions according to 10–20 system of the International Federation (Fig. 2). The first electrode setup has 30 channels covering whole brain and the second one has 15 channels covering Broca's area and Wernicke's area. Eight subjects according to two distributions are divided into two groups. Two subjects in the first group are marked by A1 and A2 respectively and six subjects in the second group are marked by B1 to B6 respectively. To measure the influence of ocular artifacts, the electrooculogram (EOG) is recorded using horizontal and vertical electrode pairs. Channel-level preprocessing is performed before applying the EOG correction, referencing the signals to left mastoid and grounding the signals to forehead. In this study, the sampling frequency is 250 Hz. A band-pass filter between 0.1 Hz and 100 Hz is used.

2.3. Feature extraction

EEG signals mainly distribute in the alpha and beta frequency ranges, so the raw signals are filtered by band-pass zero-phase filter at a range of 6–30 Hz before analysis and classification of EEG data. As a supervised method, the CSP [16] is an effective method to solve spatial filters based on the modulation of ERD/ERS. As the result of simultaneous diagonalization of the two corresponding covariance matrices, EEG signals of two different categories are projected into low-dimensional subspace by CSP spatial filters. The corresponding normalized spatial covariance matrices of trial i from classes 1 and 2 are denoted as $R_1(i)$ and $R_2(i)$, and the averaged normalized covariance matrices over trials are

$$R_1 = \frac{1}{n_1}\sum_{i=1}^{n_1} R_1(i), \quad R_2 = \frac{1}{n_2}\sum_{i=1}^{n_2} R_2(i) \tag{1}$$

R is defined as $R = R_1 + R_2$. As R is a symmetrical matrix, it can be factored into its eigenvectors: $R = U_c \lambda_c U_c^T$, where U_c is the feature vector, and λ_c is the eigenvalue of the matrix. The eigenvalues are arranged in descending order and corresponding eigenvectors are also rearranged. The whitening transformation of R is

$$P = \lambda_c^{-1/2} U_c^T \tag{2}$$

The covariance matrices R_1 and R_2 are converted to

$$S_1 = PR_1P^T, \quad S_2 = PR_2P^T \tag{3}$$

As S_1 and S_2 share the same eigenvectors, which means if $S_1 = B\lambda_1 B^T$ and then $S_2 = B\lambda_2 B^T$, and $\lambda_1 + \lambda_2 = I$. B is the common eigenvectors of S_1 and S_2, I is a unit matrix. The eigenvector with the largest eigenvalue for S_1 has the smallest eigenvalue for S_2. By the best projection matrix $W = B^T P$, we get the decomposition of each trial by transforming EEG signals X into $Z = WX$. Z has EEG source

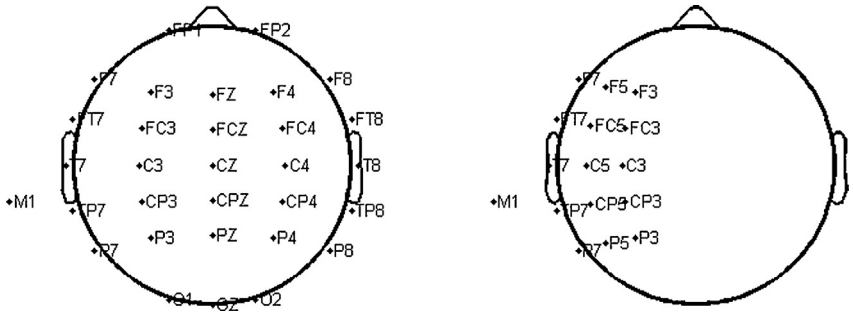

Fig. 2. Electrode positions of two EEG setups. Left electrode setup has 30 channels and right one has 15 channels, and both correspond to positions in the international 10–20 system.

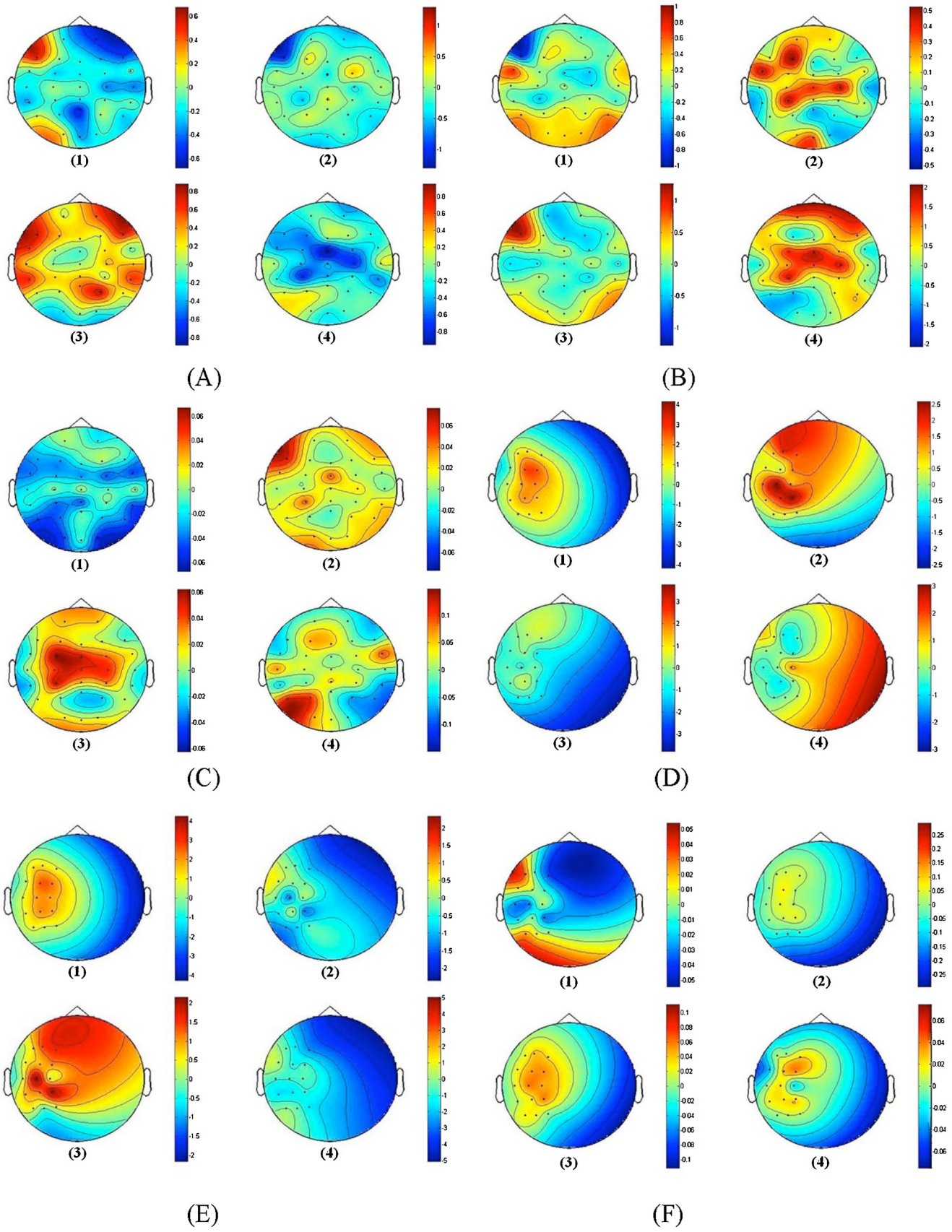

Fig. 3. The topographic maps of four most significant spatial patterns extracted by CSP method. (A)–(C) correspond to "左(left)" versus Rest, "壹(one)" versus Rest, and "左(left)" versus "壹(one)" for subject A1 respectively, and (D)–(F) correspond to "左(left)" versus Rest, "壹(one)" versus Rest, and "左(left)" versus "壹(one)" for subject B3 respectively. (1)–(4) of each subgraph are the four most significant spatial patterns.

components of different tasks, which including common and specific components, and X can be reconstructed by

$$X = W^{-1}Z \tag{4}$$

W^{-1} is the inverse matrix of W. The columns of W^{-1} are the time-invariant vectors of EEG source distribution vectors called common spatial patterns. Fig. 3 shows the four most significant common spatial patterns of subject A1 and subject B3 for "左(left)" versus Rest, "壹(one)" versus Rest, and "左(left)" versus "壹(one)" respectively.

As shown in Fig. 3, the weight values of the common spatial patterns from "左(left)" versus Rest, "壹(one)" versus Rest are larger than the weight values of "左(left)" versus "壹(one)". From here, it can be speculated that it is harder to distinguish which Chinese character is read in mind than to distinguish whether subjects are reading one character. The speculation is coincident with subsequent result.

Not all variances of the signals Z are suitable for discrimination, but a small number m of the signals are used to construct the classifier. After whitened, EEG signals are projected on the first m and last m columns eigenvectors of B. Thus, feature vectors can be calculated from signals Z_p ($p = 1,\ldots,2m$) by the following changes

$$f_p = \log\left(\frac{var(Z_p)}{\sum_{i=1}^{2m} var(Z_i)}\right) \tag{5}$$

var(·) is denoted as the variance of the vector's elements. The distributions of variance are closed to Gaussian distribution by logarithmic transformation.

2.4. Feature classification

In this study, the feature vectors of EEG signals are classified by the support vector machine (SVM) [17]. As based on statistical learning theory, SVM has many unique advantages to solve the model identification problem with small sample, nonlinear and high dimensional. It solves the problem of finding a hyperplane to separate the training data x_i with labels y_i. The distance between the boundaries of two sets i.e., the so-called "margin" is maximized, and then we can get the highest correct rate. The constraint can be written as follows

$$\begin{cases} w^T x_i - b \le -1, \forall y_i = -1 \\ w^T x_i - b \ge +1, \forall y_i = +1 \end{cases} \tag{6}$$

The primal problem of the SVM follows:

$$\min \frac{1}{2}||w||^2 \text{ subject to } y_i(w^T x_i - b) - 1 \ge 0 \,\forall i \tag{7}$$

In high dimensional model, the key of SVM classification is the choice of the kernel functions that include radial basis kernel, polynomial kernel and spline kernel. In this study, radial basis kernel is selected, and the radial basis function is

$$k(x_i, x_j) = \exp(-g||x_i - x_j||^2) \tag{8}$$

To allow mislabeled samples, error ξ and discipline factor c are introduced

$$\min \frac{1}{2}||w||^2 + c\sum_i \xi_i \text{ subject to } y_i(w^T x_i - b) - 1 + \xi_i \ge 0 \quad \xi_i \ge 0 \,\forall i \tag{9}$$

LIBSVM [18] was used to implement the SVM classifier. Fig. 4 presents to obtain the optimal values of c and g by grid search method and 10-fold cross-validation for subject B4, and the search range of c and g is from 2^{-10} to 2^{10}.

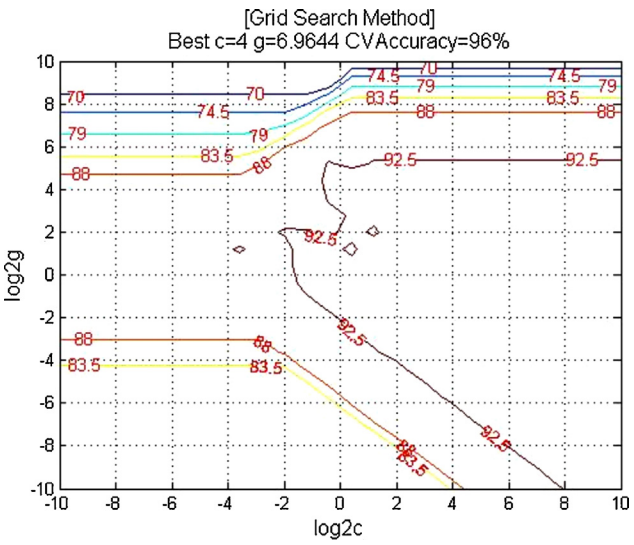

Fig. 4. The best values of c, g and accuracy for subject B4 are calculated by grid search method and 10-fold cross validation.

3. Results

In order to compare with disparity of different channels between two different speech imageries, event-related spectral perturbation (ERSP), which is superposition of single trial energy spectrum distribution, is plotted by EEGLAB [19]. As channels F7 and FC3 are near the Broca's area, and channels CP3 and P7 are near the Wernicke's area, these four channels of ERSP from subjects B1, B2 and B4 are respectively presented in Fig. 5. Each row represents the same speech imagery, and each column represents the same channel. In Fig. 5(A) and (B), the disparity of ERSPs among different channels in the same imagery is smaller than the disparity of ERSPs between different imageries in the same channel, especially for FC3 and CP3. It means that, under the same speech imagery, there is no obvious difference in energy spectrum distribution of EEG between Broca's area and Wernicke's area. Compared with motor imagery, the phenomenon is different. When imaging left hand movement, ERS will occur in motor and sensory cortex of left brain and ERD will occur in motor and sensory cortex of right brain [20]. Subject B4 is a particular example among eight subjects. When he reads each of two Chinese characters in mind, the amplitude of EEG signals in the frequency range of 10–15 Hz will become strong. The diversity between two types is not obvious.

For single-trial classification of each subject, two fragments of EEG data are analyzed. One fragment data comes from 3 s to 5 s of every trial when subjects are reading previously rendered Chinese character in mind, and another is 2 s of relax period after imagery period of each Chinese character, which is regarded as Rest. In order to judge whether EEG signals are changed when subjects read Chinese characters in mind, the signals of imagery period and Rest are used for comparison. Another reason is the purpose of asynchronous BCI systems, as the systems need to check whether the subject is performing imagery activities. To properly estimate the classification accuracy, the EEG signals of each subject are divided into training and testing sets by 10×10 cross-validation. This method randomly splits the data into ten parts. Nine of them are used to build four CSP spatial filters, extract the feature value by (5) and train the classifier. The remaining one is used to test spatial filters and classifier. Each of ten parts acts as the testing set when others are training sets. This training/testing procedure is repeated 10 times with random detachment. Table 1 presents accuracy rate.

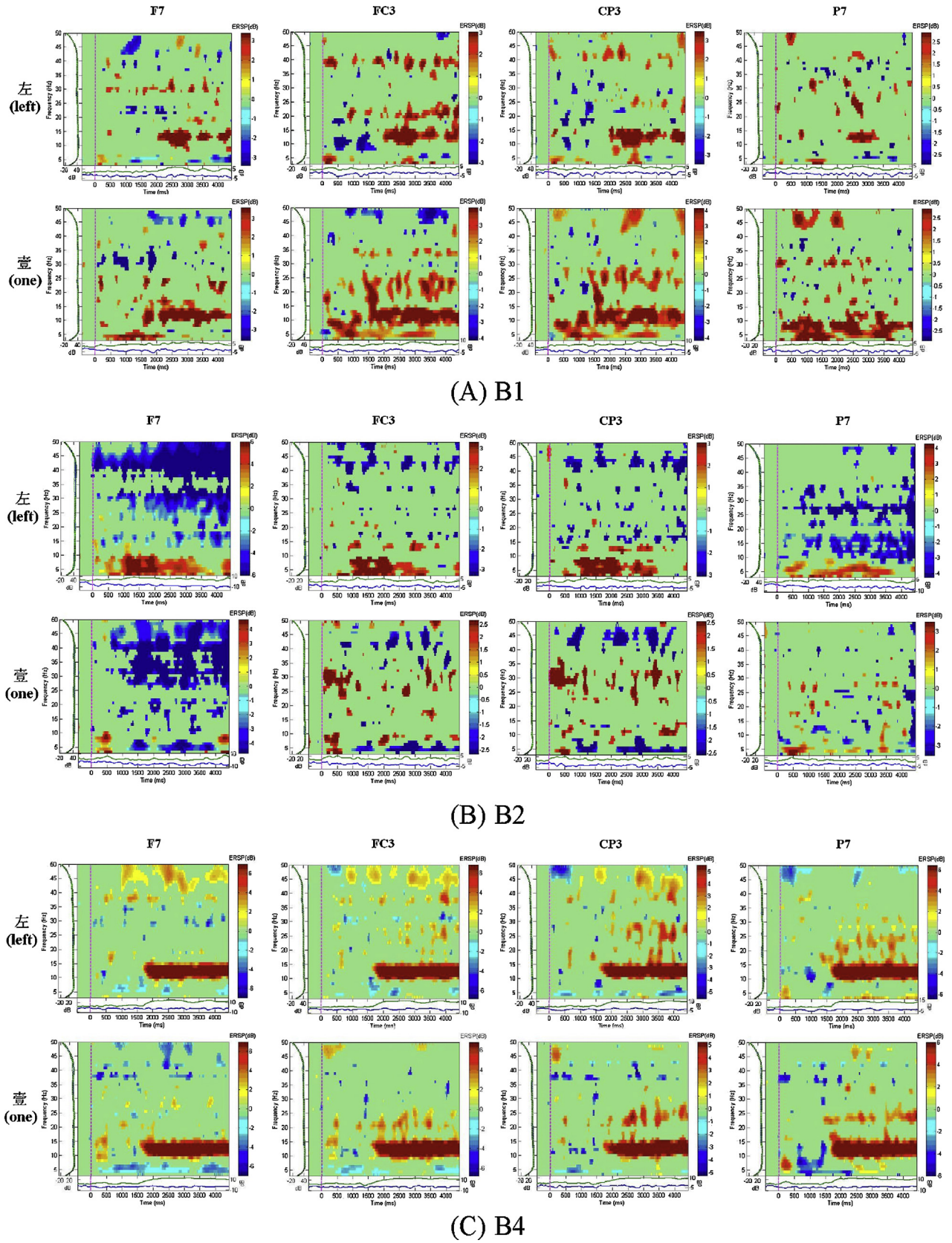

Fig. 5. ERSPs of two types of speech imagery from channels F7, FC3, CP3 and P7 for subjects B1, B2 and B4. Bootstrap significance level is 0.01, and $t = 0$ s is corresponded to $t = 1$ s in Fig. 1, when the cue appears. The horizontal axis of each subgraph shows time and the vertical axis shows frequency.

Table 1
The classification result of speech imagery EEG.

Subject	Accuracy ± std (%)		
	左(left) vs Rest	壹(one) vs Rest	左(left) vs壹(one)
A1	82.13 ± 1.56	76.34 ± 3.24	71.06 ± 2.79
A2	80.45 ± 3.34	79.26 ± 2.45	70.23 ± 2.38
B1	73.65 ± 1.98	78.45 ± 1.89	63.76 ± 3.36
B2	88.73 ± 1.67	89.78 ± 1.72	69.27 ± 1.34
B3	79.64 ± 2.35	78.95 ± 1.89	66.15 ± 2.84
B4	93.74 ± 0.97	95.76 ± 0.79	59.96 ± 1.76
B5	85.75 ± 2.78	83.02 ± 1.83	70.13 ± 3.57
B6	87.65 ± 1.38	84.19 ± 1.65	64.37 ± 2.66

As shown in Table 1, the accuracies are between 73.65% and 95.76% when determining whether subjects are reading one character in mind. The best accuracies of A1, A2, B2, B4, B5 and B6 exceed 80%. Especially for B4, the best accuracy exceeds 90%. It is also obvious to distinguish whether B4 is reading one character in mind from Fig. 5(C). For A1, A2, B3, B5 and B6, "左(left)" vs "Rest" produce higher accuracies than "壹(one)" vs "Rest", and it is just the opposite for B1, B2 and B4.

However, the accuracies of "左(left)" vs "壹(one)" are lower than other two types for eight subjects. The results of three subjects are more than 70% slightly. For B4, although it's easy to judge whether he is reading, "左(left)" vs "壹(one)" of him produces the lowest accuracy in Table 1. The ERSPs between two speech imageries are also very similar in Fig. 5(C).

4. Discussion

This study is the first to demonstrate that character speech imagery can be evolved as a control scheme for BCI. As an acquired learning skill of human, speech is an advanced perception behavior. Individual difference may vary with the acquired learning. Different languages will also bring diversity. Compared with English, Chinese is a kind of ideographic character. Therefore, from the perceptual level, the link between shape and meaning of Chinese characters may be stronger than the shape with sound. Additionally, Chinese characters are monosyllabic, and one pronunciation can express one meaning. According to [13], the average correct rate of /a/: cont from three subjects was 72.3, the average rate of /u/: cont was 75.3, and the average rate of /a/:/u/was 62.7./a/ means imagining the vocalization of /a/,/u/ means imagining the vocalization of /u/, and cont means no action. In this paper, the average correct rate of "左(left)" vs "Rest" from eight subjects is 83.97, the average rate of "壹(one)" vs "Rest" is 83.22, and the average rate of "左(left)" vs "壹(one)" is 66.87. Therefore, we have successfully classified EEG signals generated by the subjects from two periods. One period was that they were reading two Chinese characters with different shapes, pronunciations and meanings in mind and the other one was Rest. The results are better than imagining the vocalization of vowels, especially for speech imagery vs Rest.

Speech information is mainly processed by the left hemisphere of the brain, especially Broca's area and Wernicke's area. Semantic processing has a relationship with several brain areas of the left frontal lobe, and it can also monitor and extract semantic information from the posterior temporal lobes through semantic execution system [21]. In Fig. 3(A)–(C), the four most significant spatial patterns of subject A1 are calculated by CSP. These areas, where have the most significant weights, almost locate on the left hemisphere of the brain. The classification results from 15 channels covering Broca's area and Wernicke's area also perform outstanding. Some studies have shown that speech is also processed by right brain [22], but most of the best channels are covering left brain. Taking into account the practicality of BCI, the number of channels should not be too much, so it's sufficient to use the channels covering left brain. From the three aspects, we can exactly use the left hemisphere as the area to extract features from Chinese characters imagery.

As shown in Fig. 5, diversity of ERSPs among different channels in the same imagery is smaller than that between different imageries in the same channel. As a supervised method, CSP designs spatial filters by projecting EEG signals into the different imageries of Chinese characters through jointing diagonalization of the two corresponding covariance matrices. Therefore, feature vectors of EEG signals can be effectively extracted by CSP. Unsupervised algorithms, such as wavelet analysis and AR model [23], are also tried. The results are not as good as CSP. As EEG signals are changed over time with the change of users' state, adaptive algorithm [24] will be suitable.

Compared with EEG signals of motor imagery, individual differences are more significant in EEG signals of speech imagery. The reason may be that speech is a learned behavior, which relates with educational background. These findings had been studied by fMRI and ECoG [25,26]. The weight value of the common spatial patterns for channel F5 is relatively larger comparing with other channels. Furthermore, it is near the Broca's area that is related with semantic processing. To further illustrate the diversity, the energy of EEG signals for channel F5 from the same speech imagery is superimposed average in frequency domain after filtered by 6–30 Hz bandpass filter. In the frequency range of 8–15 Hz, for subjects A1, B2, B3 and B5, the energy of EEG signals as they read "左(left)" is larger than "壹(one)", but others are just the opposite. In the frequency range of 15–30 Hz, for subjects B3 and B5, the energy of EEG signals as they read "左(left)" is larger than "壹(one)", but the situation is just the opposite for B4, and the difference of others is not so obvious. The results of subjects B1, B2, B3 and B5 are shown in Fig. 6. To compare with two speech imageries of these four subjects, significance analysis is calculated by t-test. There is no significant difference in subjects B1, B2 and B3 except for B5 ($p < 0.05$).

In day-to-day life, it is common to utilize both real and imagined speech by an individual. Thus, easier operation of BCI systems will be offered by the cognitive operation. High accuracy can be achieved during the experiment though users are not trained. The advantage allows users to use this system with less training. As sensorimotor cortex, Broca's area and Wernicke's area are in different regions of the cerebral cortex, motor imagery and speech imagery will be combined to extend BCI applications in the future experiments. Potential of using the spontaneous EEG signals in BCI can be expanded from motor imagery to speech imagery for neuroprosthetic application.

From the weights of CSP spatial filters, the best performing channels of eight subjects were not exactly the same. In order to reduce the number of channels for more convenient using, the best channels will have to be chosen for each user before using the BCI systems in the future. At the beginning of the experiment, the mechanism of EEG signals from speech imagery is not entirely clear, so eigenvectors are tried to be extracted by CSP that is a state-of-the-art feature extraction algorithm for motor imagery. It is also very suitable to extract eigenvectors from two types of EEG signals. According to the results, the accuracy between two Chinese characters is not superior, so CSP spatial filters are not significantly effective for speech imagery of two Chinese characters. The reasons may be that EEG signals from imaging two Chinese characters are too similar and CSP is also very sensitive to noise and artifact. As it is more convenient to operate BCI systems by improving the accuracy, other effective algorithm of motor imagery will be learned and improved, such as multiclass CSP [27], sparse common spatial pattern (SCSP) [28] and common spatio-spectral pattern CSSP [29].

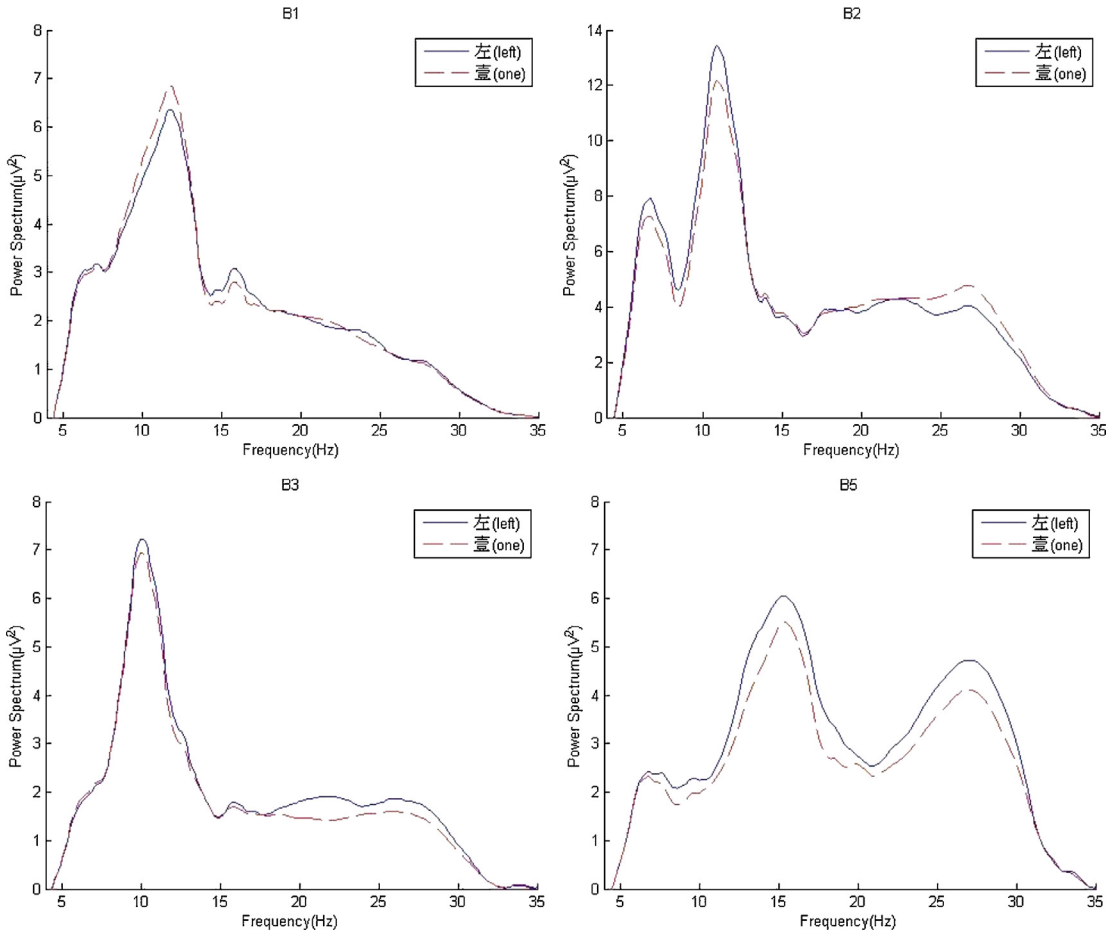

Fig. 6. Superimposed average of power spectrum in frequency domain of channel F5 for subjects B1, B2, B3 and B5. Legend '—' stands for '左(left)' and '–' stands for '壹(one)'. The waveform is smoothed by wavelet transform.

Acknowledgments

The author would like to thank the anonymous referees for valuable suggestions. This work was supported by the National Key Basic Research Program of China (No. 2010CB327705), the National High Technology Research and Development Program of China (No. 2012AA03A302), and the Fundamental Research Funds for the Central Universities under Grant CXLC12_0095, and this work was also supported by Shenzhen China Star Optoelectronics Technology Co. Ltd.

References

[1] J.R. Wolpaw, N. Birbaumer, D.J. McFarland, G. Pfurtscheller, T.M. Vaughan, Brain–computer interfaces for communication and control, Clin. Neurophysiol. 113 (2002) 767–791.
[2] C. Vidaurre, A. Schlögl, R. Cabeza, R. Scherer, G. Pfurtscheller, Adaptive on-line classification for EEG-based brain computer interfaces with AAR parameters and band power estimates, Biomed. Tech. 50 (2005) 350–354.
[3] C.E. Stepp, N. Oyunerdene, Y. Matsuoka, Kinesthetic motor imagery modulates intermuscular coherence, IEEE Trans. Neural Syst. Rehabil. Eng. 19 (2011) 638–643.
[4] T. Pistohl, A. Schulze-Bonhage, A. Aertsen, C. Mehring, T. Ball, Decoding natural grasp types from human ECoG, NeuroImage 59 (2012) 248–260.
[5] B.D. Berman, S.G. Horovitz, G. Venkataraman, M. Hallett, Self-modulation of primary motor cortex activity with motor and motor imagery tasks using real-time fMRI-based neurofeedback, NeuroImage 59 (2012) 917–925.
[6] S. Fazli, J. Mehnert, J. Steinbrink, G. Curio, A. Villringer, K.-R. Müller, B. Blankertz, Enhanced performance by a hybrid NIRS–EEG brain computer interface, NeuroImage 59 (2012) 519–529.
[7] G. Pfurtscheller, C. Brunner, A. Schlögl, F.H. Lopes da Silva, Mu rhythm (de)synchronization and EEG single-trial classification of different motor imagery tasks, NeuroImage 31 (2006) 153–159.
[8] F. Faradji, R.K. Ward, G.E. Birch, Plausibility assessment of a 2-state self-paced mental task-based BCI using the no-control performance analysis, J. Neurosci. Methods 180 (2009) 330–339.
[9] P. Lee, C. Yeh, J.Y. Cheng, C. Yang, G. Lan, An SSVEP-based BCI using high duty-cycle visual flicker, IEEE Trans. Biomed. Eng. 58 (2011) 3350–3359.
[10] M. Salvaris, C. Cinel, L. Citi, R. Poli, Novel protocols for P300-based brain–computer interfaces, IEEE Trans. Neural Syst. Rehabil. Eng. 20 (2012) 8–17.
[11] M. Naeem, C. Brunner, R. Leeb, B. Graimann, G. Pfurtscheller, Seperability of four-class motor imagery data using independent components analysis, J. Neural Eng. 3 (2006) 208–216.
[12] E.C. Leuthardt, C. Gaona, M. Sharma, N. Szrama, J. Roland, Z. Freudenberg, J. Solis, J. Breshears, G. Schalk, Using the electrocorticographic speech network to control a brain–computer interface in humans, J. Neural Eng. 8 (2011) 1–11.
[13] C.S. DaSalla, H. Kambara, M. Sato, Y. Koike, Single-trial classification of vowel speech imagery using common spatial patterns, Neural Netw. 22 (2009) 1334–1339.
[14] S.K. Scott, I.S. Johnsrude, The neuroanatomical and functional organization of speech perception, Trends Neurosci. 26 (2003) 100–107.
[15] R.L. Billingsley-Marshall, T. Clear, W.E. Mencl, P.G. Simos, P.R. Swank, D. Men, S. Sarkari, E.M. Castillo, A.C. Papanicolaou, A comparison of functional MRI and magnetoencephalography for receptive language mapping, J. Neurosci. Methods 161 (2007) 306–313.
[16] H. Ramoser, J. Müller-Gerking, G. Pfurtscheller, Optimal spatial filtering of single trial EEG during imagined hand movement, IEEE Trans. Rehabil. Eng. 8 (2000) 441–446.
[17] T.N. Lal, M. Schröder, T. Hinterberger, J. Weston, M. Bogdan, N. Bir-baumer, B. Schölkopf, Support vector channel selection in BCI, IEEE Trans. Biomed. Eng. 51 (2004) 1003–1010.
[18] C.-C. Chang, C.-J. Lin, LIBSVM: A Library for Support Vector Machines, 2011 http://www.csie.ntu.edu.tw/cjlin/libsvm
[19] A. Delorme, S. Makeig, EEGLAB: an open source toolbox for analysis of single-trial EEG dynamics, J. Neurosci. Methods 134 (2004) 9–21.
[20] Y. Jeon, C.S. Nam, Y. Kim, M.C. Whang, Event-related, (de)synchronization (ERD/ERS) during motor imagery tasks: implications for brain–computer interfaces, Int. J. Ind. Ergon. 41 (2011) 428–436.

[21] R.A. Poldrack, A.D. Wagner, M.W. Prull, J.E. Desmond, G.H. Glover, J.D.E. Gabrieli, Functional specialization for semantic and phonological processing in the left inferior prefrontal cortex, NeuroImage 10 (1999) 15–35.
[22] S. Lalande, C.M. Braun, N. Charlebois, Effects of right and left hemispheric cerebr-ovascular lesions on discrimination of prosodic and semantic aspects of affect in sentences, Brain Speech 42 (1992) 165–186.
[23] A.F. Cabrera, D. Farina, K. Dremstrup, Comparison of feature selection and classification methods for a brain–computer interface driven by non-motor imagery, Med. Biol. Eng.Comput. 48 (2010) 123–132.
[24] K.C. Veluvolu, Y. Wang, S.S. Kavuri, Adaptive estimation of EEG-rhythms for optimal band identification in BCI, J. Neurosci. Methods 203 (2012) 163–172.
[25] E.D. Palmer, H.J. Rosenc, J.G. Ojemann, R.L. Buckner, W.M. Kelley, S.E. Petersen, An event-related fMRI study of overt and covert word stem completion, NeuroImage 14 (2001) 182–193.
[26] X. Pei, E.C. Leuthardt, C.M. Gaona, P. Brunner, J.R. Wolpaw, G. Schalk, Spatiotemporal dynamics of electrocorticographic high gamma activity during overt and covert word repetition, NeuroImage 54 (2011) 2960–2972.
[27] M. Grosse-Wentrup, M. Buss, Multiclass common spatial patterns and information theoretic feature extraction, IEEE Trans. Biomed. Eng. 55 (2008) 1991–1999.
[28] M. Arvaneh, C. Guan, K.K. Ang, C. Quek, Optimizing the channel selection and classification qccuracy in EEG-based BCI, IEEE Trans. Biomed. Eng. 58 (2011) 1865–1873.
[29] S. Lemm, B. Blankertz, G. Curio, K.-R. Müller, Spatio-spectral filters for improving the classification of single trial EEG, IEEE Trans. Biomed. Eng. 52 (2005) 1541–1548.